

Regulation of Yeast Actin Behavior by Interaction of Charged Residues across the Interdomain Cleft*

Received for publication, February 19, 2002, and in revised form, March 28, 2002
Published, JBC Papers in Press, April 8, 2002, DOI 10.1074/jbc.M201685200

Xiaoyi Yao, Vinh Nguyen, Willy Wriggers‡§, and Peter A. Rubenstein¶

From the Department of Biochemistry, University of Iowa College of Medicine, Iowa City, Iowa 52242
and the ‡Department of Molecular Biology, Scripps Research Institute, La Jolla, California 92037

His⁷³ participates in the regulation of the nucleotide binding cleft conformation in yeast actin. Earlier molecular dynamics studies suggested that Asp¹⁸⁴ interacts with His⁷³ thereby stabilizing a “closed-cleft” G-actin. However, β -actin in the open-cleft state shows a closer interaction of His⁷³ with Asp¹⁷⁹ than with Asp¹⁸⁴. We have thus assessed the relative importance of Asp¹⁸⁴ and Asp¹⁷⁹ on yeast actin stability and function. Neutral substitutions at 184 or 179 alone had little adverse effect on the monomer and polymerization behavior of actin. Arg or His at 184 in H73E actin partially rescued the monomeric properties of H73E actin, as demonstrated by near-normal thermostability and wild-type (WT)-like protease digestion patterns. ATP exchange was still considerably faster than with WT-actin although slower than that of H73E alone. However, polymerization of H73E/D184R and H73E/D184H is worse than with H73E alone. Conversely, D179R rescued all monomeric properties of H73E to near WT values and largely restored polymerization rate and filament thermostability. These results and new simulations of G-actin in the “open” state underscore the importance of the His⁷³-Asp¹⁷⁹ interaction and suggest that the open and not the closed state of yeast actin may be favored in the absence of the methyl group of His⁷³.

His⁷³ is present in all actins although its function is unclear. In higher eukaryotic cells His⁷³ is post-translationally methylated on the ϵ 2 nitrogen of the imidazole ring (1, 2), although in lower eukaryotic species such as *Saccharomyces cerevisiae*, *Naegleria gruberii*, and *Candida albicans* it remains unmethylated (3, 4). The importance of this methylation is unknown. One proposed function of His⁷³, based on modeling, is that it regulates the rate of phosphate release after ATP hydrolysis during actin polymerization (5). His⁷³ is not close enough to the ATP γ -phosphate to interact directly with it prior to hydrolysis. However, after hydrolysis, the free γ -phosphate separates from the ADP and moves toward the imidazole group, allowing a possible ionic interaction to occur. This proposed interaction could retard the rate of the phosphate release from the protein interior, producing the significant lag in P_i release relative to polymerization observed with many actins. Because the release

of phosphate determines the stability of actin filament and triggers filament disassembly (6, 7), such a hypothesis, if true, would make His⁷³ an important regulator of cytoskeletal dynamics.

Results from our initial attempts to address this hypothesis suggested an important role of His⁷³ in actin structure other than the proposed phosphate release mechanism (8). We demonstrated that His⁷³ controls interdomain flexibility as well as overall stability of the actin molecule. Substitution of His⁷³ with a neutral or acidic residue resulted in an increased interdomain flexibility and decreased thermal stability indicated by faster ATP exchange rate, increased susceptibility to selected proteases, and decreased melting temperature. In contrast, increasing the positive charge by replacement with Arg or Lys leads to a hyperstable monomer structure with decreased interdomain flexibility and increased thermal stability.

A model for the conformational determination by His⁷³ has been proposed by Wriggers and co-workers (8) based on the molecular simulations of WT,¹ H73R, and H73E mutant actins. That model is based on the closed-cleft muscle actin structure that has methylhistidine at position 73 (9). The methyl group was removed to simulate the WT state of yeast actin. The results suggest that His⁷³ is constrained with residue Asp¹⁸⁴ across the cleft in a manner dependent on the methylation or protonation state of the imidazole ring. When methylhistidine is present, the imidazole group is about 5 Å away from the carboxylate of Asp¹⁸⁴, stabilized by a hydrogen bond between the δ 1 proton and the Gly¹⁵⁸ oxygen. Without the methyl group, the imidazole group has three possible protonation states, with protons at either δ 1 or ϵ 2 nitrogens or both. When the δ 1 nitrogen alone is protonated, the local conformation observed was the same as that when methylhistidine is present. When ϵ 2 nitrogen alone is protonated, the imidazole ring is predicted to flip over and form a cross-domain interaction with Asp¹⁸⁴ leading to a distinct conformation not possible with methylhistidine based on steric considerations. Although this contact with Asp¹⁸⁴ did not completely form in the doubly protonated His⁷³ case, probably because of an undersampling of the conformational variability in a single simulation trajectory, it appeared that His⁷³-Asp¹⁸⁴ interactions based on ϵ 2 protonation could provide a new mechanism for cross-domain stabilization. This new conformation has not yet been observed crystallographically. If true, it distinguishes yeast actin from muscle actin that has methylhistidine, and the difference might account, at least partially, for some of the differences in behavior of these two actins (10, 11). This cross-domain interaction is disrupted in our severest mutant, H73E, in which Glu⁷³ actually forms an interaction with Arg¹⁸³ in a different direction, causing a rearrangement of the set of hydrogen bonds at the bottom of the

* This work was supported in part by Grant GM33689 from the National Institutes of Health (to P. A. R.). The costs of publication of this article were defrayed in part by the payment of page charges. This article must therefore be hereby marked “advertisement” in accordance with 18 U.S.C. Section 1734 solely to indicate this fact.

§ Supported in part by Grant P41RR12255 from the National Institutes of Health.

¶ To whom correspondence should be addressed: Dept. of Biochemistry, University of Iowa College of Medicine, Iowa City, IA 52242. Tel.: 319-335-7911; Fax: 319-335-9570.

¹ The abbreviation used is: WT, wild type.

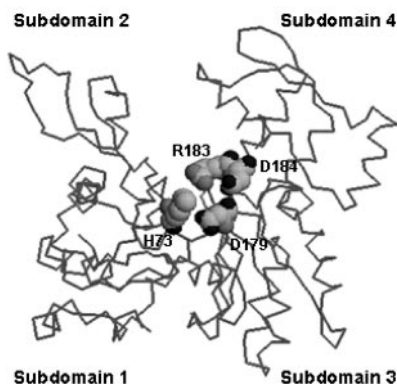


FIG. 1. Monomeric nonmuscle β -actin in the open conformation. Residues His⁷³, Asp¹⁷⁹, Asp¹⁸⁴, and Arg¹⁸³ are labeled.

cleft. This reorientation may well lead to the abnormal monomer and polymer behavior we observe.

An alternative scenario became apparent when we examined the actin structure in a more open state. The modeling study, predicting a cross-domain interaction between His⁷³ and Asp¹⁸⁴, was based on an actin structure in the closed state that was observed in the earlier crystal structures (9). However, Schutt and co-workers (12) more recently crystallized actin in an open-cleft conformation by altering the conditions for crystal bathing. Due to the opening of the cleft, His⁷³ moves away from Asp¹⁸⁴ causing a separation of ~ 8 Å between the side chains of His⁷³ and Asp¹⁸⁴, a distance that appears to disfavor a direct contact. Asp¹⁷⁹, which in the closed state is parked below His⁷³ further down in the cleft, now faces His⁷³ with the carboxyl group about 4 Å away from the imidazole ring. Thus, the 73–184 cross-cleft interaction in the closed state, strongly suggested by modeling, could be replaced by a 73–179 interaction in the open conformation. A structure depicting the relationship of these residues is shown in Fig. 1. These two forms of interaction might be important in maintaining the distinct cleft conformation associated with the two states. His⁷³ would be the pivotal residue involved in both interactions.

In this paper, in order to test the role of Asp¹⁸⁴ and Asp¹⁷⁹ in determining the conformation of actin, we used site-directed mutagenesis to assess the effects of compensatory substitutions in this collection of residues on monomer stability and polymerizability. Because the conformational sampling by molecular dynamics is limited to the structural vicinity of one actin isoform, we performed new mutant structure predictions starting from both the closed and open states. Together, both mutagenesis and modeling allowed us to reexamine the role of Asp¹⁸⁴ and Asp¹⁷⁹ on structure and function of yeast actin.

MATERIALS AND METHODS

The site-directed mutagenesis kit was purchased from Stratagene. Oligodeoxynucleotides used for site-directed mutagenesis were obtained through the DNA Core Facility at the University of Iowa. DNase I was obtained from Worthington. Affi-Gel 10 and Micro Bio-Spin P-30 Tris gel filtration chromatography columns were obtained from Bio-Rad. 1,N⁶-Ethenoadenosine 5'-triphosphate, α -chymotrypsin, trypsin, and subtilisin were purchased from Sigma. All other compounds used were reagent grade quality.

Deoxyoligonucleotide-directed Mutagenesis and Generation of Mutant Yeast Cells—Site-directed mutagenesis was used to introduce the desired mutations into the yeast actin coding sequence. The template plasmid for single substitution was pRS314WN (13), a derivative of pRS314 (14) carrying a WT yeast actin coding sequence and promoter between the BamHI and EcoRI sites. Double mutations H73E/D184R, H73E/D184H, and H73E/D179R were produced using pRS314-H73E actin as the template (8). The oligodeoxynucleotide 5'-CGATTGGCCCGTAGAG(A/C)C(T/A/G)T(C/A)TTGACTGACTACTTGATGAAG-3' was used to generate the mutant actins in which the codon for 184 Asp(GAT) was mutated to that for Ala(GCT), Val(GTT), Asn(AAC),

His(CAC), and Arg(AGA). The oligodeoxynucleotide 5'-CGCCATTTTG-AGAATCAG(A)A(T)TTGGCCGGTAGAGATTGAC-3' was used to generate the mutant actins in which the codon for Asp¹⁷⁹(GAT) was mutated to Arg(AGA) and Asn(AAT). The underlined sequences are the mutated codons. The DNA was sequenced in each case to verify the desired mutation.

Plasmids containing the mutant coding sequences were introduced into a *trp1*, *ura3-52* haploid cell in which the chromosomal *ACT1* gene had been disrupted by replacement of the coding sequence with the *LEU2* gene. Wild-type actin was expressed in these recipient cells from another centromeric plasmid containing the *URA3* gene. Following transformation with the mutant plasmid and selection on tryptophan-deficient medium, surviving cells were subjected to plasmid shuffling to eliminate the plasmid carrying the WT-actin gene. The mutant plasmid was rescued from surviving *trp*⁺, *ura*⁻ cells and sequenced to ensure that the mutation was still intact. Viable cells were readily obtained for all mutants.

Purification of Yeast Wild-type, Asp¹⁸⁴, and Asp¹⁷⁹ Mutant Actins—Wild-type, Asp¹⁸⁴, and Asp¹⁷⁹ mutant actins were purified using a combination of DNase I affinity chromatography, DEAE-cellulose chromatography, and subsequent polymerization-depolymerization cycling as described previously (15). Ca²⁺-G-actin was stored in Ca²⁺-G-buffer (10 mM Tris-HCl, pH 7.5, 0.2 mM CaCl₂, 0.2 mM ATP, and 0.5 mM dithiothreitol). Ca²⁺-actin was converted to the Mg²⁺ form by treatment with 50 μ M EGTA in the presence of 0.1 mM MgCl₂ at 25 °C for 5 min as modified from Chen and Rubenstein (16) and Pollard (17). Mg²⁺-G-actin was used immediately after the conversion from Ca²⁺-G-actin. Actins were stored at 4 °C following purification and used within 4 days following completion of purification.

Actin Polymerization—Actin polymerization was assessed by the increase in light scattering that occurs following the addition of 2 mM MgCl₂ and 50 mM KCl to a G-actin solution in the thermostated cuvette chamber of a Spex Fluorolog 3 fluorescence spectrometer. Excitation and emission wavelengths were set at 360 nm. For all experiments, wild-type actin was run as a control, and experiments were repeated with at least two different batches of actins. To assess cold sensitivity, actin was polymerized at 25 °C until a plateau was reached. The temperature was then lowered to 4 °C over 15–30 min, and the sample was subsequently maintained at this temperature during which the change in light scattering was monitored. For the cold-reversed polymerization assay, the temperature was then raised back to 25 °C, and the change in the light scattering signal was followed.

Critical Concentration Determination—G-actin was polymerized by the addition of 2 mM MgCl₂ and 50 mM KCl at 25 °C for 2 h. F-actin was then diluted to the desired concentration with F buffer (G buffer plus 2 mM MgCl₂ and 50 mM KCl) and further incubated at 25 °C for 1 h. The light scattering of F-actin at each concentration was monitored as described above. The light scattering from G-actin at each concentration was also determined. The net increase in light scattering (F-G) was plotted as a function of actin concentration. The apparent critical concentration was obtained by adding a linear trend line to the data points and by determining the intercept on the x axis.

Thermal Denaturation—The apparent melting temperatures of the wild-type and mutant G-actins were determined by circular dichroism according to Chen *et al.* (18). 1.4 μ M G-actin was heated at a constant rate of 1 °C/min over a range from 20 to 80 °C with constant stirring of the samples over the entire range tested. Changes in the ellipticity of actin samples were monitored at 222 nm in an AVIV 62 DS spectropolarimeter. Data were fitted to a two-state model with a single transition between a native and a denatured form of the protein, and the *T_m* value was defined as the temperature when 50% of the G-actin was in the denatured form.

Nucleotide Exchange—Unbound ATP was removed from a 20 μ M G-actin solution using a Micro Bio-Spin P-30 column (Bio-Rad), and the actin was incubated with 0.3 mM 1,N⁶-ethenoadenosine 5'-triphosphate at 4 °C for 2 h. Excess nucleotide was removed using a Micro Bio-Spin P-30. The subsequent actin solution was diluted with ATP-free G buffer to 3 μ M. The exchange was triggered by the addition of 0.1 mM cold ATP to 3 μ M labeled actin. The decay in fluorescence that accompanied release of the etheno nucleotide from the actin was monitored as a function of time with excitation and emission wavelengths at 340 and 410 nm, respectively. Nucleotide exchange rates were derived by fitting the data to a single exponential expression.

Electron Microscopy—Polymerized actin at 25 °C was applied to carbon-coated Formvar grids and visualized following negative staining with 1.5% (w/v) uranyl acetate using a Hitachi 7000 electron microscope (University of Iowa Electron Microscope Facility).

Limited Proteolysis of G-actin—Alterations in the tertiary structure

TABLE I
T_m values (°C) of Asp¹⁸⁴ and Asp¹⁷⁹ mutant actins

The thermal stability of Asp¹⁸⁴ and Asp¹⁷⁹ mutant actins was assessed by subjecting G-actin solutions to increasing temperatures and monitoring the circular dichroism of the samples at 222 nm as a function of temperature as described under "Materials and Methods." The *T_m* value for each actin was obtained by fitting the change in dichroism to a two-state denaturation model with the help of Dr. B. Sorensen. The assay was repeated with two actin preparations, and the average *T_m* values with variations between the two are listed in the table. The *T_m* values of H73E were determined (8), and the values listed in this table were adjusted based on relative values of the WT-actin due to a calibration of the temperature probe of the CD instrument.

	WT	H73E	H73E/D184H	H73E/D184R	H73E/D179R	D179N	D179R
Mg ²⁺ -actin	53 ± 0.2	44 ± 0.3	50 ± 0.4	50 ± 0.2	53 ± 0.4	55 ± 0.2	55 ± 0.2
Ca ²⁺ -actin	61 ± 0.4	55 ± 0.3	61 ± 0.5	59 ± 0.5	61 ± 0.2	63 ± 0.3	63 ± 0.2

of G-actins were monitored by the susceptibility of the actins (9 μM) to limited digestion by the following three enzymes at the indicated actin/protease ratios (w/w): trypsin (80:1), subtilisin (600:1), and chymotrypsin (16:1) essentially as described previously (19). Incubations were carried out at room temperature for the desired time. The digestion with trypsin was stopped with 10 μg/ml trypsin inhibitor, and the digestion with the other two proteases was stopped with 1 mM phenylmethylsulfonyl fluoride. The samples were then separated by electrophoresis on a 12% SDS-polyacrylamide gel, and the fragments were visualized by staining with Coomassie Blue.

Molecular Modeling Studies—Simulated annealing refinements of modeled Mg²⁺-ATP actin mutants in the closed state were carried out as described (8) using the program X-PLOR (25). The mutants were modeled by adding or replacing atoms of the respective side chains. Actin in the closed state was simulated with the His⁷³ proton at the ε2 nitrogen, a conformation that was found earlier to depart from the crystallographic conformation exhibited by methylhistidine actin after forming a salt bridge with Asp¹⁸⁴ (8). The simulated systems also included 1,159 water molecules that provided a solvent shell for the exposed surface of the molecule (5). β-Actin in the open state with methylhistidine and unmethylated histidine was simulated similarly using 1,232 water molecules starting from the crystal structure (12). To explore a possible interaction between Asp¹⁷⁹ and His⁷³ in the open-cleft conformation, His⁷³ was simulated in two protonation states, one with a proton at the ε2 nitrogen (as in closed actin), and the other in an alternative, doubly protonated His⁷³⁺ state.

RESULTS

Neutral Substitution of Asp¹⁸⁴ Minimally Affects Actin Monomeric Structure and Causes Mild Defects in Polymerization

Our earlier modeling suggested an His⁷³-Asp¹⁸⁴ cross-domain interaction in yeast actin (8). To test this hypothesis, we first replaced Asp¹⁸⁴ with two neutral aliphatic residues with different bulk, Ala and Val, and Asn a neutral residue isosteric with Asp. The effects of the mutations on the monomeric structure of actin were determined based on thermal denaturation, protease digestion, and ATP exchange assay. All the mutants showed similar melting temperatures with a difference of less than 1 °C from that of WT-actin (data not shown). Controlled proteolysis with trypsin, subtilisin, or α-chymotrypsin as a probe of the conformation of the top of subdomain 2 produced a WT-like digestion pattern for all of the mutants (data not shown). The rate of exchange of bound ATP with free ATP, related to central cleft conformation, was also determined. Ala and Val had the same rate as WT-actin. Asn exhibited a slightly (25%) faster exchange than WT-actin (data not shown). These results demonstrated that the neutral substitutions of Asp¹⁸⁴ affected actin monomeric structure to a much lesser extent than did the His⁷³ neutral substitutions, suggesting a limited role of a 73–184 interaction in conformational regulation.

We next determined the effects of the single mutations on the polymerization properties of actin. The mutations did not alter the polymerization rate dramatically (data not shown). Ala and Val polymerized at a rate similar to that of WT-actin, and Asn appeared to polymerize slightly more slowly. All three mutations had higher critical concentrations for polymerization (1.0

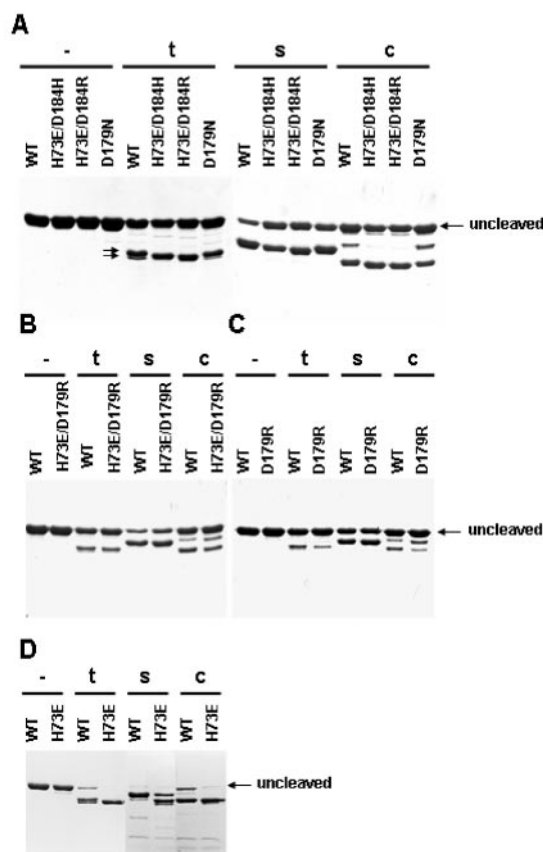


FIG. 2. Protease susceptibility of Asp¹⁸⁴ and Asp¹⁷⁹ mutant actins. WT, H73E/D184H, H73E/D184R, D179N, D179R, and H73E/D179R actins in the Ca²⁺-G form were subjected to controlled proteolysis by trypsin, subtilisin, or α-chymotrypsin as described under "Materials and Methods." After digestion, the samples were separated by electrophoresis on 12% SDS-polyacrylamide gels. A, WT, H73E/D184H, H73E/D184R, and D179N actins. The two arrows indicate the differences in the trypsin digestion patterns between WT, H73E/D184H, and H73E/D184R. B, WT and H73E/D179R actins. C, WT and D179R actins. D, WT and H73E actins, published previously (8). The assay was repeated with two actin preparations, and the same results were obtained at each time.

μM as compared with 0.5 μM in WT-actin). The cold resistance of the mutant actin filaments was also tested. All three mutant actins showed very mild depolymerization at 4 °C indicated by a 15–25% drop in the light scattering signal (WT-actin drops 5–10%), and the disassembly was reversible. Electron microscopy confirmed WT-looking filament formation from both the standard and cold-reversed polymerization assays.

D184R or D184H Partially Restores the Altered Properties of H73E Monomeric Actin to a More WT State

Although removal of the charge on 184 did not have a dramatic negative effect on monomer structure, it was possible

that neighboring residues somehow compensated for the defects in order to maintain a WT-like conformation. Based on the significant defect associated with the H73E mutation, we next assessed the effects of planting a positively charged residue at 184 in the H73E mutant actin. This would recreate the original ionic interaction but in an inverted orientation. If such an interaction were a major factor in actin behavior, this second substitution might be expected to convert H73E to a more normal phenotype.

Table I shows that indeed D184H and D184R partially restored the overall thermal stability of H73E actin. Whereas monomeric H73E actin had a T_m of 55 °C in the Ca²⁺ form and 45 °C in the Mg²⁺ form, the double mutants H73E/D184H and H73E/D184R showed increased T_m values of 61 and 59 °C respectively in the Ca²⁺ form. In the Mg²⁺ form, the T_m values of both the double mutants increased to 50 °C.

Results from selective protease digestion studies as a probe of actin structure indicated that H73E caused a significant conformational change in the top of subdomain 2 leading to a much more extensive digestion pattern than that observed for WT-actin (8). The addition of a positive charge at 184 largely reversed this defect (Fig. 2A). However, the conformations of subdomain 2 in the double mutants were still different from that of WT-actin as indicated by more extensive digestion by trypsin and α -chymotrypsin (arrows in Fig. 2A).

H73E dramatically enhanced the rate of ATP exchange suggesting a much more flexible interdomain cleft conformation. Fig. 3 shows the results of the second substitution on the effect of ATP exchange, and the $t_{1/2}$ values for each reaction are summarized in Table II. Although H73E/D184R or H73E/D184H retarded the rate of ATP exchange by 3- or 4-fold compared with H73E alone, their rates were still significantly faster than that of WT-actin.

D184R or D184H Amplifies the Polymerization Defect of H73E Actin

H73E polymerizes much more slowly compared with WT-actin and shows a lower extent of polymerization as well,

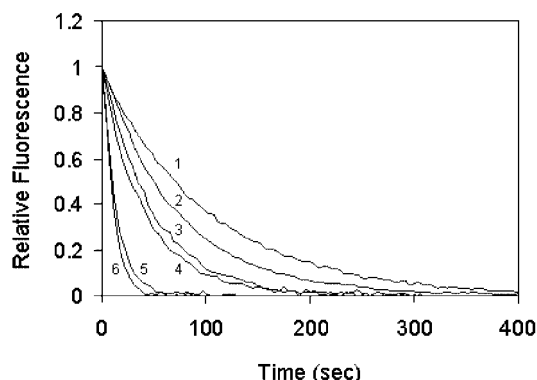


FIG. 3. ATP exchange in Asp¹⁸⁴ and Asp¹⁷⁹ mutant actins. These mutant actins in the Ca²⁺ form were assessed for their ability to exchange bound 1,N⁶-ethenoadenosine 5'-triphosphate for unbound ATP by monitoring the fluorescence of the bound ϵ -nucleotide as a function of time as described under "Materials and Methods." Curve 3, WT-actin; curve 5, H73E/D184R; curve 6, H73E/D184H; curve 4, H73E/D179R; curve 1, D179R; curve 2, D179N.

TABLE II
 $t_{1/2}$ values for ϵ -ATP exchange with Asp¹⁸⁴ and Asp¹⁷⁹ mutant actins

The exchange data for actins as shown in Fig. 3 were fitted to a first-order decay plot and the $t_{1/2}$ values calculated. The experiment was repeated with two different batches of actin. The average values with the variations are shown.

	WT	H73E	H73E/D184H	H73E/D184R	H73E/D179R	D179N	D179R
Mg (s)	37 ± 3	2.4 ± 0.2	7 ± 0.5	10 ± 1	29 ± 2	50 ± 4	71 ± 2

because of a higher critical concentration (8). Although the second mutation at 184 partially rescued the monomeric defects associated with H73E actin, to our surprise, the second mutant exacerbated the polymerization defect observed with H73E alone. The rates of polymerization of H73E/D184R and H73E/D184H were even slower than H73E. More significantly, the extent of polymerization was much less than H73E (Fig. 4). The critical concentrations for polymerization of H73E/D184R and H73E/D184H were 3.3 and 2.7 μ M, respectively, whereas H73E had a critical concentration of 0.9 μ M (Fig. 5 and Table III).

The mutations at residue 184 also increased the cold sensitivity associated with H73E actin polymerization. At 9 μ M, only half of the H73E filaments disassembled at 4 °C, and H73E/D184R and H73E/D184H completely disassembled under the same conditions (Fig. 6A). Complete disassembly was also observed with the two double mutant actins at a higher actin concentration of 14 μ M (data not shown). However, Fig. 6B shows this disassembly could be reversed by elevating the temperature to 25 °C. EM confirmed filament reformation at 25 °C (data not shown).

D179N Causes No Adverse Effects on Monomeric Structure and Polymerization

Because the results from Asp¹⁸⁴ single mutations and His⁷³/Asp¹⁸⁴ double mutations did not fully support a strong 73–184 interaction, we tested the alternative prediction involving an interaction between His⁷³ and Asp¹⁷⁹ favored in the more open actin conformation.

We first made the D179N single substitution to assess the inherent importance of this residue. No adverse changes were caused by the mutation based on the same assays used above. The protease digestion pattern shows no difference from that of WT-actin (Fig. 2A). Table I shows that D179N exhibited a melting temperature slightly higher than that of the WT-actin, suggesting increased stability. Consistent with this result, a slower ATP exchange was also observed with D179N (Fig. 3 and Table II). Surprisingly, D179N polymerized slightly faster than WT-actin (Fig. 7A), and the critical concentration for polymerization was 0.2 μ M, lower than WT-actin (Fig. 8 and Table III). D179N polymerization was not

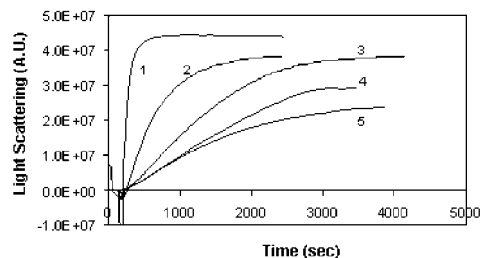


FIG. 4. Polymerization of H73E/D184R, H73E/D184H, and H73E/D179R mutant actins at 25 °C. Polymerization of the Ca²⁺ form of each of the mutant and WT-actins was induced by the addition of salt to the appropriate 9 μ M G-actin solutions as described under "Materials and Methods." The increase in light scattering due to polymerization was followed as a function of time. Curve 1, WT-actin; curve 2, H73E/D179R; curve 3, H73E; curve 4, H73E/D184H; curve 5, H73E/D184R. This experiment was repeated with two different batches of actin with essentially the same results.

cold-sensitive, in contrast to polymerization of D184N actin (data not shown).

D179R Significantly Rescues the Monomeric Structure and Polymerization Defects of H73E Actin

We next converted Asp¹⁷⁹ to Arg in H73E actin in order to recreate a potentially reversed ionic interaction involving H73E, similar to what we had done with D184R. As in the case for D184R, the D179R also rescued the monomeric features of the Glu mutant but to a much greater degree. The T_m value of H73E/D179R was the same as WT-actin (Table I). The protease accessibility was the same as WT-actin for all three proteases used (Fig. 2B). Moreover, the ATP exchange rate of this double mutant was greatly retarded compared with that of H73E (Fig. 3). It had a $t_{1/2}$ of 29 s, much closer to the WT-actin than were those of the Asp¹⁸⁴ double mutants (Table II). Even more surprising, unlike D184R, D179R restored the polymerization behavior of H73E to a more WT situation. The polymerization rate of H73E/D179R was increased compared with the H73E mutant alone (Fig. 4). The stability of the H73E/D179R filaments at low temperature was also significantly increased. With 9 μM polymerized H73E/D179R actin at 4 °C, ~25% of the filaments disassembled compared with the 50% disassembly observed with H73E alone and 100% observed with H73E/D184R (Fig. 6).

D179R Single Mutation Causes No Adverse Effects on Monomer Structure and Mild Defects in Polymerization

The results from H73E/D179R strongly suggest that an ionic interaction between 73 and 179 is important for actin behavior as indicated by monomer features as well as polymerization properties, consistent with the proximity of the side chains in the open structure of actin. Because substitution of Asp¹⁷⁹ with Asn in WT-actin resulted in an enhanced polymerization with a faster rate and lower critical concentration, we wanted to determine whether the polymerization rescue by D179R in the Glu⁷³ mutant was due to the effect of mutation at 179 position by itself or dependent on the Glu⁷³-Arg¹⁸⁴ interaction. Therefore, a single D179R substitution was made in the WT-actin. The monomer behavior of D179R was very similar to that of D179N, showing a slightly higher T_m as well as a slower ATP exchange rate compared with WT-actin (Fig. 3, Table I, and

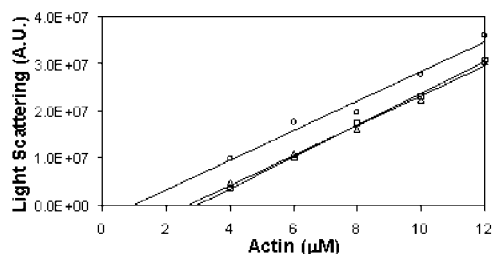


FIG. 5. **Apparent critical concentration determination of Asp¹⁸⁴ and Asp¹⁷⁹ mutant actins.** The net increase in light scattering by polymerization of 4, 6, 8, 10, and 12 μM actin was determined as described under “Materials and Methods” and plotted as a function of actin concentration. \circ , H73E/D179R; Δ , H73E/D184H; \square , H73E/D184R. The apparent critical concentration was determined by the intersection of each linear trend line with the x axis and is shown in Table III. The assay was repeated with two actin preparations.

Table II). However, unlike D179N, the polymerization of D179R was slightly defective with a slower rate than WT-actin (Fig. 7A) and a small degree of cold sensitivity at 4 °C (Fig. 7B). The critical concentration for D179R polymerization was essentially the same as WT-actin (Fig. 8 and Table III). Thus, the rescue of the polymerization defect of H73E by D179R could not have been due solely to the improvement imposed upon the WT structure by the D179R mutation alone.

Molecular Modeling of WT, D179R, D179N, H73E/D184R, and H73E/D179R Actins

Histidine and Methylhistidine WT-actin in the Closed and Open Conformation—In the studies performed here based on the closed actin conformation, WT His⁷³ was simulated in the singly, ϵ 2-protonated state that favored a salt bridge with Asp¹⁸⁴ (Fig. 9A) as shown in our earlier simulations. A tunneling through the ϵ 2-protonated state toward a salt bridge with Asp¹⁸⁴ was expected also for doubly protonated His⁷³⁺ based on pK_a considerations (8). One would expect that the favorable electrostatics of doubly protonated His⁷³⁺ would facilitate such a salt bridge, but the contact in the His⁷³⁺ case did not form completely (8). A re-examination of the original model of His⁷³⁺ actin (Fig. 9B) shows that two ordered water molecules prevented the direct contact. It is well known among practitioners of molecular dynamics that the relatively long residence times of ordered water molecules might lead to an under sampling of available conformations in the short (ps to ns) simulation times (5). Therefore, the forming of a salt bridge is a statistical event.

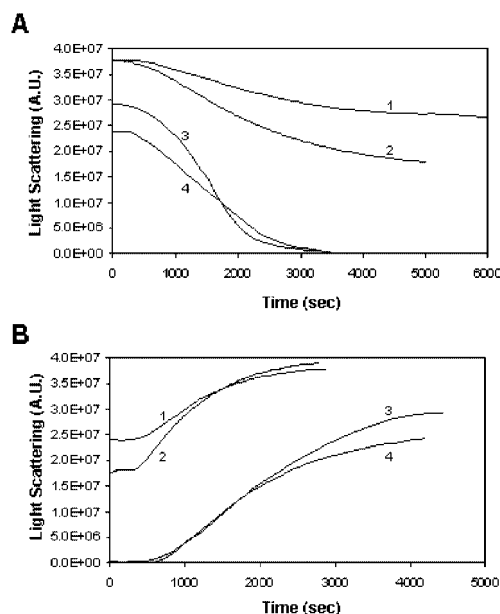


FIG. 6. **Cold-induced depolymerization of Asp¹⁸⁴ and Asp¹⁷⁹ mutant actins.** A, cold-induced depolymerization assay of double mutant actins. H73E/D179R (curve 1), H73E (curve 2), H73E/D184H (curve 3), and H73E/D184R (curve 4). Mutant actins (9 μM) were polymerized at 25 °C. The temperature was then lowered to 4 °C, and the light scattering was monitored over time. B, repolymerization assay. Following cold-induced depolymerization, the temperature was returned to 25 °C, and the increase in light scattering due to repolymerization was monitored. The curves are numbered as described in A.

TABLE III
Critical concentrations (μM) of Asp¹⁸⁴ and Asp¹⁷⁹ mutant actins

These data were derived from the experiments shown in Fig. 5 and Fig. 8. The numbers are an average of two independent experiments with different preparations of actin. The ranges of the measurements are shown in each case as well.

WT	H73E	H73E/D184H	H73E/D184R	H73E/D179R	D179N	D179R
0.45 ± 0.05	0.9 ± 0.2	2.7 ± 0.1	3.4 ± 0.1	0.9 ± 0.1	0.2 ± 0.05	0.5 ± 0.1

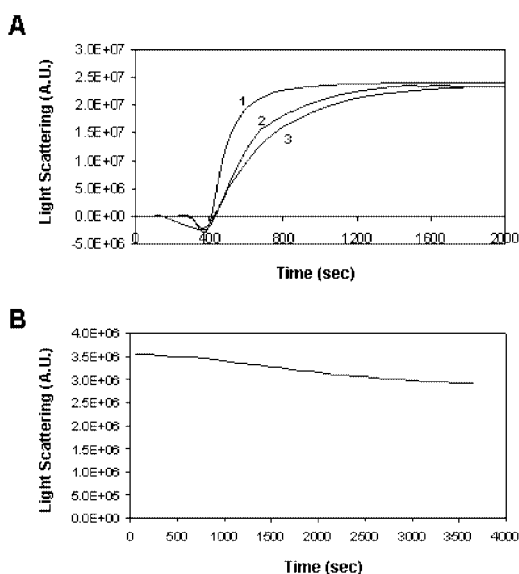


FIG. 7. Polymerization of Asp¹⁷⁹ single mutant actins at 25 °C. A, polymerization of D179N (curve 1), D179R (curve 3), and WT (curve 2)-actins was induced by the addition of salt to the appropriate 4.5 μM G-actin solutions. The increase in light scattering due to polymerization was followed as a function of time. B, D179R was polymerized at 25 °C. The temperature was then lowered to 4 °C, and the light scattering was monitored over time.

Here, we report all ordered water molecules (see “Materials and Methods”) whenever they reside between two salt bridge candidates, because they might point to a functionally relevant interaction.

Simulations with WT His⁷³ in β -actin in the open form are shown in Fig. 10. Once the methyl group is removed, ϵ 2-protonated His⁷³ is again able to move into an “in line” configuration with Asp¹⁸⁴ (Fig. 10, B and C). In open actin the separation of methyl-free His⁷³ to Asp¹⁸⁴ is surprisingly small, 3.7 and 3.4 Å, for His⁷³ (Fig. 10B) and His⁷³⁺ (Fig. 10C), respectively, but a direct contact (as observed in closed actin; Fig. 9A) does not form due to the opening of the overall polypeptide fold in the vicinity. The interactions of methyl-free His⁷³ do not vary significantly with the protonation state, except for an electrostatic contact with Asp¹⁷⁹ that is slightly favored by charged His⁷³⁺ (Fig. 10C). His⁷³ is attracted by Asp¹⁷⁹ despite the suboptimal alignment of the side chains that face opposing directions. Although not a typical example, there is a hydrogen bond between unmethylated His⁷³ with one of the Asp¹⁷⁹ oxygens (hydrogen-acceptor distances 2.6 and 2.5 Å, for His⁷³ and His⁷³⁺, respectively). The 73–179 interaction is not observed in the closed state or with methylhistidine in the open state.

Asp¹⁸⁴ and Asp¹⁷⁹ Mutations in WT and H73E Background—In our earlier model of the H73E mutant based on the closed state conformation (8), Glu⁷³ interacted strongly with Arg¹⁸³ and electrostatically repelled Asp¹⁸⁴ (Fig. 7F in Ref. 8) and, similarly, Asp¹⁷⁹ (not shown). In all other substitutions of His⁷³ discussed in Ref. 8 with various protonation states and Arg, Asp¹⁷⁹ remained in place similar to the situation with the Me-His⁷³ crystal conformation. It is interesting that only the H73E mutant had an effect on the Asp¹⁷⁹ position and also that H73E favored a strong salt bridge with Arg¹⁸³, an interaction that was not observed in any other structure. Therefore, we wished to explore the effect of substitutions at positions 184 and 179 both in a WT and a H73E background and to monitor the effect of the substitutions specifically on the side chains of Arg¹⁸³ and position 179 that were sensitive to the earlier H73E substitution. To this end, we performed four additional molec-

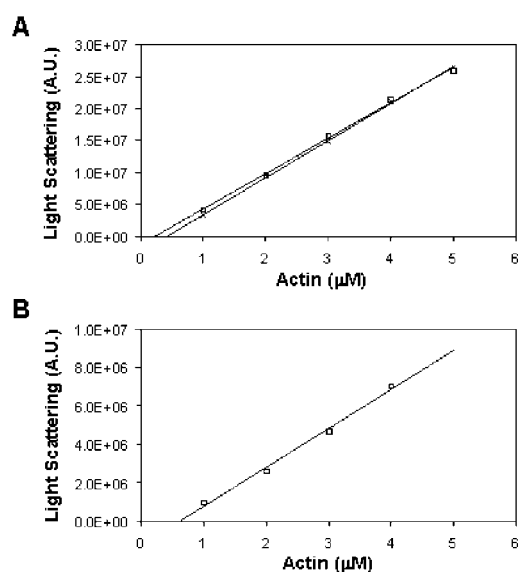


FIG. 8. Apparent critical concentration determination of Asp¹⁷⁹ single mutant actins. The net increase in light scattering by polymerization of 1–5 μM actin was determined as described under “Materials and Methods” and plotted as a function of actin concentration. A, WT-actin (\times); D179N (\square). B, D179R. The apparent critical concentration was determined by the intercept of each linear trend line on the x axis. The assay was repeated with two actin preparations.

ular dynamics refinements that elucidate the behavior of the mutants relative to the earlier models.

Fig. 9, C and D, shows the effects of Arg and Asn substitutions at position 179 on WT-actin. In the D179R mutant, Arg¹⁷⁹ forms a salt bridge with Asp¹⁸⁴ (hydrogen acceptor distances, 2.2 and 2.8 Å; donor hydrogen acceptor angles, 50 and 3°) and thereby prevents a direct cross-domain contact of His⁷³ with Asp¹⁸⁴. Substitution with Asn at position 179 has very little effect on the structure; His⁷³ is oriented toward Asp¹⁸⁴ (separation 5.1 Å), but the forming of a direct salt bridge is prevented by three ordered water molecules, similar to the earlier simulation with His⁷³⁺ (Fig. 9B).

The effect of Arg substitutions at positions 184 and 179 on a H73E background is presented in Fig. 9, E and F. Substitution by Arg¹⁸⁴ results in an inversion of charges at the putative 73–184 salt bridge relative to WT (Fig. 9E). However, the inversion of the charges does not result in an equivalently inverted salt bridge. The presence of positive charges at both Arg¹⁸³ and Arg¹⁸⁴ bends Glu⁷³ away from Arg¹⁸⁴ toward Arg¹⁸³. A hydrogen bond is observed with the extended side chain of Arg¹⁸⁴ (hydrogen acceptor distance, 1.7 Å; donor hydrogen acceptor angle, 12°), but in addition, Glu⁷³ interacts with the side chain of Arg¹⁸³ (separation 4.2 Å), so that it no longer provides an exclusive structural restraint on cross-domain interactions via a contact with position 184. Substitution to Arg¹⁷⁹ (Fig. 9F) results in two direct hydrogen bonds between Arg¹⁷⁹ and Glu⁷³ (hydrogen acceptor distances, 1.7 and 2.1 Å; donor hydrogen acceptor angles, 16 and 26°). In addition, Arg¹⁷⁹ interacts with Asp¹⁸⁴ (separation 4.1 Å) through three ordered water molecules (Fig. 9F). Therefore, Arg¹⁷⁹ rescues a stabilizing cross-domain contact between positions 73 and 184.

As with the closed form, a strong interaction between Glu⁷³ and Arg¹⁷⁹ is also observed from simulations based on the open conformation. Fig. 10D shows that in the H73E/D179R mutant, a salt bridge is formed between 73 and 179 (distance 1.7 Å and angle 21°).

DISCUSSION

The conserved His⁷³ is part of a group of ionic residues near the base of the cleft separating the two domains of actin. We

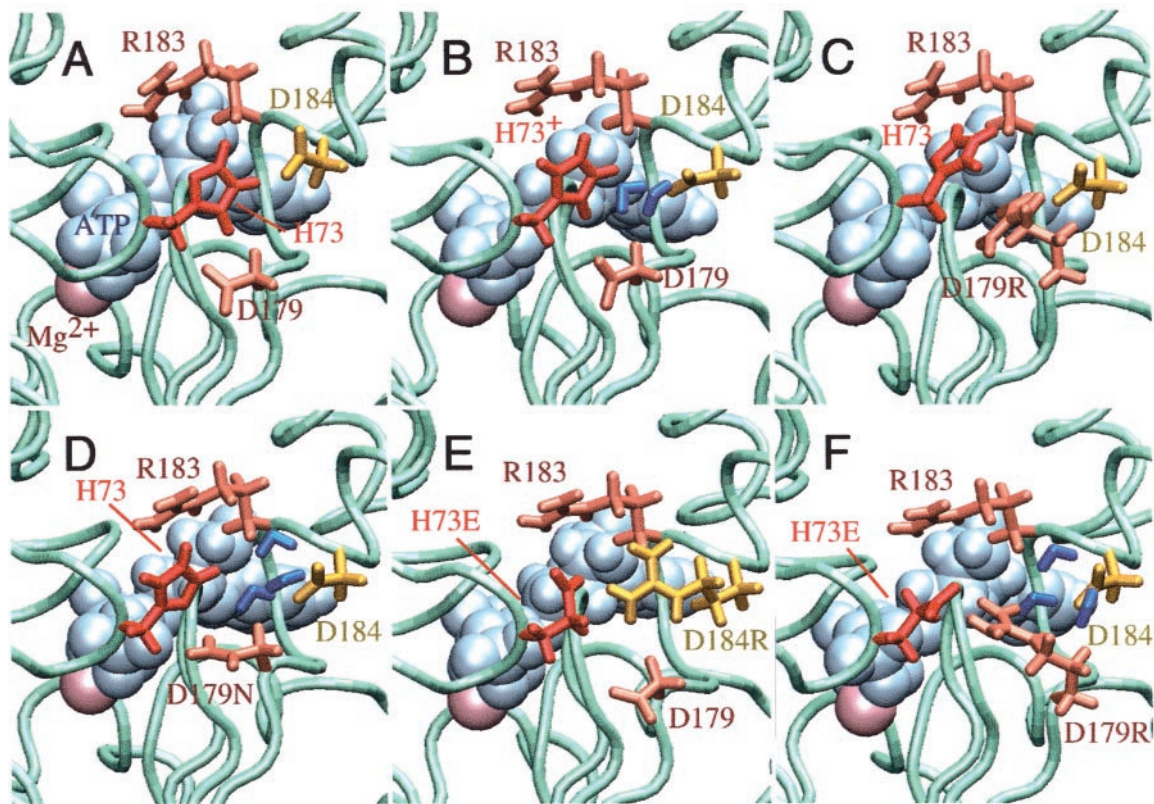


FIG. 9. Structural models of actin in the vicinity of the nucleotide binding region in the interdomain cleft depicting the effects of substitutions at His⁷³, Asp¹⁷⁹, and Asp¹⁸⁴ in closed actin. Molecular dynamics simulations based on the closed conformation of muscle actin were performed as described previously (8). *A*, unmethylated His⁷³ (proton at $\epsilon 2$ nitrogen) forms a salt bridge with Asp¹⁸⁴ (8); *B*, two bridging water molecules prevent a direct contact of doubly protonated His⁷³⁺ with Asp¹⁸⁴ (8); *C*, D179R substitution; *D*, D179N substitution; *E*, “inverted salt bridge” H73E and D184R; *F*, substitutions H73E and D179R. Figs. 9 and 10 were generated using the program VMD (25). The structures in Figs. 9 and 10 can be viewed at the following site: <ftp.scripps.edu/pub/wriggers/yao02>.

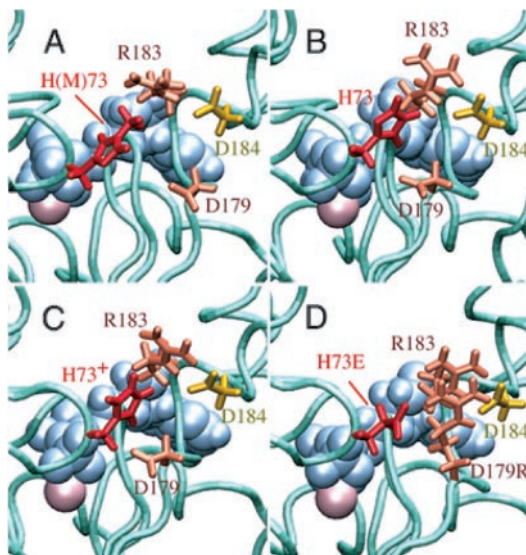


FIG. 10. Structural models based on the open cleft conformation of β -actin. *A*, the control model starting from the crystal structure with methylated His⁷³; *B*, unmethylated His⁷³ (proton at $\epsilon 2$ nitrogen) interacts with Asp¹⁸⁴ and Asp¹⁷⁹; *C*, doubly protonated (unmethylated) His⁷³⁺ interacts with Asp¹⁸⁴ and Asp¹⁷⁹; *D*, H73E/D179R actin.

wished to define the role of this residue in controlling actin monomer flexibility and polymerizability. The combination of site-directed mutagenesis experiments and MD modeling studies we performed allowed us to gain novel insight into two aspects of yeast actin function. First is the possible propensity of yeast actin for the open *versus* the closed state in a manner

that might involve the methylation state of His⁷³. Second is the identification of specific residues with which the residue at position 73 might interact within this larger group of ionic species. These are based on the most effective compensatory change that results in the rescue of abnormal behavior brought about by substitution of His⁷³ with glutamate.

Open Versus the Closed State—Page and co-workers (20) had described previously an “open” conformation for β -nonmuscle actin to go along with the “closed” conformation originally observed. According to these authors (20), this conformational switch results mainly from a rotation of the connecting residues between the two domains including loop 333–338 and helix 137–145. These residues are almost identical between β -non-muscle actin and yeast actin. The only difference is that in yeast actin, the two terminal residues of the helix are Ser, whereas in the higher actin they are Ala.

Two lines of experimental evidence have suggested that yeast actin might be more likely than the higher eukaryotic actins to assume this open state. One such type of behavior is the fact that yeast actin exchanges nucleotide 10 times faster (21), polymerizes more rapidly, and does not display the lag in releasing phosphate following hydrolysis of the bound adenine nucleotide that occurs concomitantly with polymerization (22). Next, in EM reconstruction experiments performed by Egelman and colleagues (10), a major difference between muscle actin and yeast F-actin was decreased density or a more open conformation in yeast actin in the region of the interdomain cleft at or near where the nucleotide is bound. Our modeling results suggest that in the absence of the His⁷³ methyl group, the imidazole ring of the histidine is able to flip over and form a new conformation involving a potential strong ionic

bond with Asp¹⁷⁹ in the open conformation, an interaction that is not possible because of steric constraints when the methyl group on the histidine is present. When the actin moves to the closed state, Asp¹⁷⁹ inserts into the space below His⁷³, precluding the interaction of these two residues and favoring instead a hydrogen bond between His⁷³ and Asp¹⁸⁴. If this postulated interaction between His⁷³ and Asp¹⁷⁹ plays a substantial role in stabilizing the open conformation of actin, then yeast actin might be more likely than the higher actins to exist in this open state.

Rescue of the H73E Phenotype—The rationale underlying our mutagenesis study was that if a particular ionic interaction were important for protein function, disruption of that interaction might be deleterious, and restoration of the ionic pair in an inverted configuration should rescue the defective phenotype. Our modeling studies also provide a potential explanation for our observation of an enhanced ability of an arginine residue at position 179 instead of one at position 184 to more effectively rescue the defects associated with an H73E mutation, especially in terms of actin polymerizability. In the closed conformation, where residues at positions 73 and 184 are in close proximity, Glu⁷³ would be potentially able to interact with cationic residues at both 183 and 184 in the double mutant. This is a different situation than in wild-type actin where His⁷³ would only be expected to interact with Asp¹⁸⁴. Thus, an arginine at position 184 in the double mutant would have to compete with that at position 183, resulting in a situation where it is unlikely that the Glu at position 73 would be returned to a position in the cleft close to the situation in the WT conformation.

In contrast, a positively charged arginine at position 179 in the double mutant is stabilized in its contact with Glu⁷³ by Asp¹⁸⁴. Hence, competition for Glu⁷³ by Arg¹⁸³ is much less likely to occur, especially if in yeast actin the open conformation is favored which would encourage the formation of the Glu⁷³-Arg¹⁷⁹ interaction. The result would be an actin with a much more normal conformation and behavior properties, precisely the result we observe.

The mild cold-sensitive polymerization behavior observed with the Asp¹⁸⁴ single mutants and the intensified cold-sensitive polymerization behavior observed with the Glu⁷³/Arg¹⁸⁴ double mutant strongly suggests that a second factor exists in the failure of introduction of Arg at position 184 to rescue the Glu⁷³ mutant. Asp¹⁸⁴ is near a subdomain 3/4 loop with a hydrophobic tip. This loop has been proposed to play a significant role in stabilization of the actin filament by forming a cross-strand interaction with a hydrophobic pocket consisting partially of residues in actin subdomain 2 near and possibly

controlled by His⁷³ (23). We had shown previously that mutations in the hydrophobic portion of this loop *per se* also produce cold-sensitive polymerization behavior (13, 24) as did mutating His⁷³ itself (8). Thus, in the case of the Glu⁷³/Arg¹⁸⁴ double mutant, the failure to rescue the Arg⁷³ phenotype may result from an alteration in the proposed plug-pocket interaction due to a simple introduction of a charge change at position 184 in addition to incomplete restoration by Arg¹⁸⁴ of the cleft residues to a more WT configuration.

In summary, together with our initial work on the role of His⁷³ in actin function, our results suggest a structural basis for what appears to be a propensity of yeast actin to assume a more open conformation than actins from higher eukaryotic organisms and the potential importance of the absence of histidine methylation in this behavior. The double mutant studies further begin to allow one to differentiate the importance of possible cross-cleft interactions in dictating actin behavior and perhaps provide the first solution evidence for the assumption of the open state by actin.

REFERENCES

- Asatoor, A. M., and Armstrong, M. D. (1967) *Biochem. Biophys. Res. Commun.* **26**, 168–174
- Johnson, P., Harris, C. I., and Perry, S. V. (1967) *Biochem. J.* **105**, 361–370
- Kalhor, H. R., Niewmierzyccka, A., Faull, K. F., Yao, X., Grade, S., Clarke, S., and Rubenstein, P. A. (1999) *Arch. Biochem. Biophys.* **370**, 105–111
- Sussman, D. J., Sellers, J. R., Flicker, P., Lai, E. Y., Cannon, L. E., Szent-Gyorgyi, A. G., and Fulton, C. (1984) *J. Biol. Chem.* **259**, 7349–7354
- Wriggers, W., and Schulten, K. (1999) *Proteins* **35**, 262–273
- Carlier, M. F. (1990) *Adv. Biophys.* **26**, 51–73
- Pollard, T. D., Blanchoin, L., and Mullins, R. D. (2001) *J. Cell Sci.* **114**, 3–4
- Yao, X., Grade, S., Wriggers, W., and Rubenstein, P. A. (1999) *J. Biol. Chem.* **274**, 37443–37449
- McLaughlin, P. J., Gooch, J. T., Mannherz, H. G., and Weeds, A. G. (1993) *Nature* **364**, 685–692
- Orlova, A., Chen, X., Rubenstein, P. A., and Egelman, E. H. (1997) *J. Mol. Biol.* **271**, 235–243
- Kim, E., Miller, C. J., and Reisler, E. (1996) *Biochemistry* **35**, 16566–16572
- Chik, J. K., Lindberg, U., and Schutt, C. E. (1996) *J. Mol. Biol.* **263**, 607–623
- Chen, X., Cook, R. K., and Rubenstein, P. A. (1993) *J. Cell Biol.* **123**, 1185–1195
- Cook, R. K., Sheff, D. R., and Rubenstein, P. A. (1991) *J. Biol. Chem.* **266**, 16825–16833
- Cook, R. K., Blake, W. T., and Rubenstein, P. A. (1992) *J. Biol. Chem.* **267**, 9430–9436
- Chen, X., and Rubenstein, P. A. (1995) *J. Biol. Chem.* **270**, 11406–11414
- Pollard, T. D. (1986) *J. Cell Biol.* **103**, 2747–2754
- Chen, X., Peng, J., Pedram, M., Swenson, C. A., and Rubenstein, P. A. (1995) *J. Biol. Chem.* **270**, 11415–11423
- Kuang, B., and Rubenstein, P. A. (1997) *J. Biol. Chem.* **272**, 4412–4418
- Page, R., Lindberg, U., and Schutt, C. E. (1998) *J. Mol. Biol.* **280**, 463–474
- Miller, C. J., Cheung, P., White, P., and Reisler, E. (1995) *Biophys. J.* **68**, S50–S54
- Yao, X., and Rubenstein, P. A. (2001) *J. Biol. Chem.* **276**, 25598–25604
- Holmes, K. C., Popp, D., Gebhard, W., and Kabsch, W. (1990) *Nature* **347**, 44–49
- Kuang, B., and Rubenstein, P. A. (1997) *J. Biol. Chem.* **272**, 1237–1247
- Brunger, A. T. (1992) *X-PLOR: A System for X-ray Crystallography and NMR*, Version 3.1, Yale University, New Haven, CT